The FASEB Journal article fj.10-162438. Published online August 18, 2010.

Acetaminophen, *via* its reactive metabolite *N*-acetyl-*p*-benzo-quinoneimine and transient receptor potential ankyrin-1 stimulation, causes neurogenic inflammation in the airways and other tissues in rodents

Romina Nassini,*,[1] Serena Materazzi,*,[1] Eunice Andrè,*,[2] Laura Sartiani,* Giancarlo Aldini,[§] Marcello Trevisani,[‖] Chiara Carnini,[¶] Daniela Massi,[†] Pamela Pedretti,* Marina Carini,[§] Elisabetta Cerbai,* Delia Preti,[#] Gino Villetti,[¶] Maurizio Civelli,[¶] Gabriela Trevisan,* Chiara Azzari,[‡] Susan Stokesberry, Laura Sadofsky,[††] Lorcan McGarvey,** Riccardo Patacchini,[¶] and Pierangelo Geppetti*,[3]**

*Department of Preclinical and Clinical Pharmacology, [†]Department of Human Pathology and Oncology, and [‡]Department of Pediatrics, University of Florence, Florence, Italy; [§]Department of Pharmaceutical Sciences, University of Milan, Milan, Italy; [‖]Pharmeste Srl, Ferrara, Italy; [¶]Pharmacology Department, Chiesi Farmaceutici SpA, Parma, Italy; [#]Department of Pharmaceutical Chemistry, University of Ferrara, Ferrara, Italy; **Centre for Infection and Immunity, Queen's University Belfast, Belfast, UK; and [††]Division of Cardiovascular and Respiratory Studies, University of Hull, Castle Hill Hospital, Hull, UK

ABSTRACT **Acetaminophen [*N*-acetyl-*p*-aminophenol (APAP)] is the most common antipyretic/analgesic medicine worldwide. If APAP is overdosed, its metabolite, *N*-acetyl-*p*-benzo-quinoneimine (NAPQI), causes liver damage. However, epidemiological evidence has associated previous use of therapeutic APAP doses with the risk of chronic obstructive pulmonary disease (COPD) and asthma. The transient receptor potential ankyrin-1 (TRPA1) channel is expressed by peptidergic primary sensory neurons. Because NAPQI, like other TRPA1 activators, is an electrophilic molecule, we hypothesized that APAP, *via* NAPQI, stimulates TRPA1, thus causing airway neurogenic inflammation. NAPQI selectively excites human recombinant and native (neuroblastoma cells) TRPA1. TRPA1 activation by NAPQI releases proinflammatory neuropeptides (substance P and calcitonin gene-related peptide) from sensory nerve terminals in rodent airways, thereby causing neurogenic edema and neutrophilia. Single or repeated administration of therapeutic (15–60 mg/kg) APAP doses to mice produces detectable levels of NAPQI in the lung, and increases neutrophil numbers, myeloperoxidase activity, and cytokine and chemokine levels in the airways or skin. Inflammatory responses evoked by NAPQI and APAP are abated by TRPA1 antagonism or are absent in TRPA1-deficient mice. This novel pathway, distinguished from the tissue-damaging effect of NAPQI, may contribute to the risk of COPD and asthma associated with therapeutic APAP use.—Nassini, R., Materazzi, S., Andrè, E., Sartiani, L., Aldini, G., Trevisani, M., Carnini, C., Massi, D., Pedretti, P., Carini, M., Cerbai, E., Preti, D., Villetti, G., Civelli, M., Trevisan, G., Azzari, C., Stokesberry, S., Sadofsky, L., McGarvey, L., Patacchini, R., Geppetti, P. Acetaminophen, *via* its reactive metabolite *N*-acetyl-*p*-benzo-quinoneimine and transient receptor potential ankyrin-1 stimulation causes neurogenic inflammation in the airways and other tissues in rodents. *FASEB J.* 24, 000–000 (2010). www.fasebj.org**

Key Words: primary sensory neurons · substance P · asthma · chronic obstructive pulmonary disease

Acetaminophen [paracetamol, *N*-acetyl-*p*-aminophenol (APAP)] is one of the most popular analgesic/antipyretic medicines worldwide, and it has almost completely replaced the use of aspirin in infants to avoid the risk of Reye's syndrome (1). In overdose, APAP causes severe liver damage *via* a toxic metabolite, *N*-acetyl-*p*-benzo-quinoneimine (NAPQI) (2), but it is safe at therapeutic doses. However, in the past 10 yr a wide series of epidemiological studies has shown that exposure to therapeutic doses of APAP during intrauterine life, infancy (3), and childhood (4) and in adults (5–7) is one of the risk factors for asthma (8, 9) and chronic obstructive pulmonary disease (COPD)

[1] These authors contributed equally to this work.

[2] Current address: Department of Biophysics and Pharmacology, Universidade Federal do Rio Grande do Norte, Natal, Brazil.

[3] Correspondence: Department of Preclinical and Clinical Pharmacology, University of Florence, Viale Pieraccini 6, 50139 Florence, Italy. E-mail: geppetti@unifi.it

doi: 10.1096/fj.10-162438

(7). A recent cross-sectional study (10) on 205,487 children aged 6–7 yr in 31 developed and developing countries has provided further evidence that the use of APAP during the first year of life or current use of APAP in childhood is robustly associated with a dose-dependent, increased risk of asthma, eczema, and rhinoconjunctivitis in the exposed children. NAPQI, generated through a P450 cytochrome-oxidative pathway, is normally inactivated by glutathione (GSH) conjugation, forming the 3′-glutathionyl-*S*-yl-APAP adduct (3′-GS-APAP) (11). GSH consumption by NAPQI has been proposed as one possible mechanism by which APAP increases the risk of asthma, because GSH-depleted lungs would no longer be protected against oxidative stress (3, 8, 10, 12, 13). However, evidence in support of this hypothesis has not yet been provided, and the precise mechanism by which APAP increases the risk of asthma and allergic diseases remains unknown.

The transient receptor potential ankyrin-1 (TRPA1) cation channel is coexpressed by a subset of nociceptive primary sensory neurons with the "capsaicin receptor," TRPV1 (14, 15). TRPV1 or TRPA1 stimulation in peripheral terminals of primary sensory neurons releases the neuropeptides calcitonin gene-related peptide (CGRP) and substance P (SP), which mediate neurogenic inflammatory responses (16). Neurogenic inflammation encompasses hyperemia, plasma protein extravasation, mediator release, and leukocyte infiltration and has been thought to contribute to a series of inflammatory diseases, including asthma and COPD (17). A number of TRPA1 agonists, including the α,β-unsaturated aldehydes, acrolein (18) and 4-hydroxy-2-nonenal (19), possess an electrophilic carbon atom that undergoes nucleophilic attack by the cysteine residues of proteins. This mechanism, which results in the formation of stable proteic adducts (20), is considered responsible for TRPA1 stimulation (21).

NAPQI, like other TRPA1 activators, is a highly electrophilic and reactive compound (22). Therefore, we hypothesized that NAPQI activates the TRPA1 channel. We also hypothesized that exposure of mice to APAP doses equivalent to the therapeutic doses used in humans results in TRPA1-dependent neurogenic inflammation. Our findings indicate that NAPQI selectively activates TRPA1 and that therapeutic doses of APAP, *via* NAPQI generation and TRPA1 stimulation, cause neurogenic inflammation in the rodent airways.

MATERIALS AND METHODS

Reagents

If not otherwise indicated, all reagents were from Sigma-Aldrich (Milan, Italy). NAPQI was dissolved in 100% DMSO (final concentration 50 mM) and stored at −80°C. No color change or decreased efficacy was observed in NAPQI stocks. For *in vivo* administration, APAP was dissolved in 5% DMSO in isotonic saline solution, warmed to 37°C for intraperitoneal administration, and in 20% Solutol HS (BASF Chemical Co., Ludwigshafen, Germany) in distilled water for intragastric administration. The TRPA1 selective antagonist, HC-030031, has been synthesized as reported previously (23). For *in vitro* experiments, HC-030031 was dissolved in 100% DMSO (1 mM stock solution) and further diluted in aqueous buffer solution. For *in vivo* experiments, HC-030031 was prepared in 0.5% carboxymethylcellulose (CMC). The tachykinin NK_2 receptor antagonist, SR48968, was kindly donated by X. Emonds-Alt (Sanofi-Aventis, Montpellier, France).

Animals

Institutional animal care and use committees of the University of Florence approved all procedures. Dunkin-Hartley guinea pigs (male, 250 g; Charles River, Milan, Italy), Sprague-Dawley rats (male, 250 g) and C57BL/6 mice (male, 25 g) (Harlan Laboratories, Milan, Italy), and wild-type ($Trpa1^{+/+}$) or TRPA1-deficient mice ($Trpa1^{-/-}$), generated by heterozygous mice on a C57BL/6 background (18), were housed in a temperature- and humidity-controlled vivarium (12-h light-dark cycle; free access to food and water). Experiments with $Trpa1^{+/+}$ and $Trpa1^{-/-}$ littermate mice were masked to the genotype. Animals were euthanized with a high dose of sodium pentobarbital (200 mg/kg i.p.).

Cell culture and isolation of primary sensory neurons

Human embryonic kidney (HEK) cells transfected with the cDNA of the rat TRPA1 (rTRPA1-HEK293) or with the empty vector (vector-HEK293), generated and grown as reported previously (24), were kindly donated by N. W. Bunnett (University of California, San Francisco, CA, USA). HEK293 cells stably transfected with human TRPA1 (hTRPA1-HEK293), kindly donated by A. H. Morice (University of Hull, Hull, UK), were cultured as described previously (25). HEK293 cells transfected with human TRPV1 (hTRPV1-HEK293), the kind gift of Martin J. Gunthorpe (GlaxoSmithKline, Harlow, UK), were grown as described previously (26). The human neuroblastoma cell line, IMR-32 (American Type Culture Collection, Manassas, VA, USA), has been reported (27) to undergo remarkable differentiation in response to treatment with 5-bromo-20-deoxyuridine (BrdU), a phenomenon that is associated with expression of TRPA1. Thus, we adopted the same procedure to express TRPA1 in IMR-32 cells by adding 5 μM BrdU to the medium for 8–12 d (27) before performing calcium imaging experiments. Rat jugular ganglion (JG) and mouse dorsal root ganglion (DRG) were isolated and cultured as described previously (23).

Cellular recording

For calcium fluorescence measurements, cells were loaded with Fura-2,AM ester (5 μM; Alexis Biochemicals, Lausen, Switzerland), and changes by the F_{340}/F_{380} ratio were recorded with a dynamic image analysis system (Laboratory Automation 2.0; RC Software, Florence, Italy) as described previously (23). Cells were exposed to APAP, NAPQI, capsaicin, cinnamaldehyde, activating peptide (SLIGKV-NH_2) of the human PAR-2 receptor (hPAR-2 AP), carbachol, or their vehicles, which were 0.1% DMSO, 0.2% DMSO, 0.01% ethanol, 0.1% DMSO, and distilled water, respectively. HC-030031 and capsazepine vehicles (used in all the *in vitro* experiments) were 1% DMSO and 0.1% DMSO, respectively. JG and DRG cells were challenged with capsaicin to identify primary

sensory neurons. Results are expressed as a percentage of the maximum response to ionomycin (5 μM).

TRPA1 current was detected as inward current activated on cell superfusion with NAPQI, cinnamaldehyde, and capsaicin to identify primary sensory neurons. Peak current was normalized with respect to cell membrane capacitance (pA/pF). The experimental setup for patch-clamp recording and data acquisition, similar to that described previously (28), was performed using the whole-cell configuration of the patch-clamp technique with a glass-borosilicate pipette that had a resistance of 2–3 MΩ when filled with the internal solution (CsCl, 110 mM; $MgCl_2$, 3 mM; MgATP, 3 mM; EGTA, 10 mM; and HEPES, 10 mM; pH 7.2, adjusted with CsOH). Electrophysiological recordings were performed using a microsuperfusor, which allowed rapid changes of the solution bathing the cell (120 mM NaCl, 5 mM KCl, 2 mM $MgCl_2$, 5 mM $CaCl_2$, 10 mM HEPES, and 10 mM glucose, pH 7.4, adjusted with NaOH), kept at room temperature (~25°C). Cell membrane capacitance was measured by applying a ±10 mV pulse starting from a holding potential of −70 mV; values were calculated by integrating the capacitive currents elicited by step potentials and used to compute current densities. Current was evoked in the voltage-clamp mode by a step potential at −80 mV; signals was sampled at 50 kHz and filtered at 10 kHz.

Neuropeptide release

Rat airways were removed, and slices (~0.4 mm) were prepared at 4°C using a tissue slicer (McIlwain tissue chopper; Mickle Laboratory Engineering, Guildford, Surrey, UK). Slices (100 mg) were placed in 1-ml chambers and superfused with oxygenated (95% O_2/5% CO_2) Krebs' solution (119 mM NaCl, 25 mM $NaHCO_3$, 1.2 mM KH_2PO_4, 1.5 mM $MgSO_4$, 2.5 mM $CaCl_2$, 4.7 mM KCl, and 1 mM D-glucose) maintained at 37°C and containing 0.1% BSA, 1 μM phosphoramidon, and 1 μM captopril. After a 90-min stabilization period, NAPQI or its vehicle was added for 10 min. In some experiments, slices were perfused with a Ca^{2+}-free medium, containing 1 mM EDTA, or afferent nerves were desensitized and depleted of neuropeptides by preincubation with 10 μM capsaicin for 20 min before stimulation. The 10-min fractions that were collected (2 before, 1 during, and 1 after exposure to the stimulus) were analyzed for CGRP and SP immunoreactivities by enzyme immunoassays, as described previously (23). NAPQI (150 μM) did not cross-react with SP (Cayman Chemical, Ann Arbor, MI, USA) or CGRP (the kind gift of C. Creminon, CEN-Saclay, Gif-sur-Yvette, France) antisera. Detection limits of the assays were 5 pg/ml for CGRP and 2 pg/ml for SP. Results are expressed as femtomoles of peptide per gram of tissue per 20 min.

Airway motor responses

Motor responses in isolated guinea pig bronchial rings were studied as reported previously (23). The results are expressed as a percentage of the maximum response induced by carbachol (1 μM). For the measurement of pulmonary insufflation pressure (PIP), guinea pigs were anesthetized with sodium pentobarbital (60 mg/kg i.p.), and a plastic cannula was inserted into the trachea after tracheotomy to facilitate respiration. Animals were artificially ventilated (60 breaths/min) through a rodent ventilator (Ugo Basile, Varese, Italy). PIP was monitored continuously with a bronchospasm transducer (Ugo Basile) connected to a side arm to the tracheal cannula. Intravenous pancuronium bromide (0.06 mg/kg) was administered to each animal to prevent spontaneous respiratory movements. After tracheal intubation, guinea pigs were allowed to recover for 30 min to stabilize the PIP basal level (29). NAPQI (1 mM, 200 μl) or its vehicle (2% DMSO in isotonic saline) were administered through the intratracheal route, by inserting a 30-gauge needle just below the tip of the cannula. Some animals were pretreated with buthionine sulfoximine (BSO; 600 mg/kg i.p.) to inhibit γ-glutamylcysteine synthetase, thereby depleting cells of GSH (30) or its vehicle (isotonic saline) 1 h before NAPQI administration. In another experimental set, animals were treated with APAP (300 mg/kg i.p.) or its vehicle (5% DMSO in warmed isotonic saline) and 90 min later were challenged with acetylcholine (50 nmol/kg i.v.). HC-030031 [200 mg/kg intragastrically (i.g.)] or its vehicle (0.5% CMC i.g.) was administered 60 min before NAPQI or APAP injections. Data are expressed as percent increase in PIP over baseline.

Plasma protein extravasation

Anesthetized (sodium pentobarbital, 50 mg/kg i.p.) rats were injected with Evans blue dye (30 mg/kg i.v.) 1 min before intratracheal (200 μl) or conjunctival (10 μl) instillation of NAPQI (1 mM) or its vehicle (2% DMSO in isotonic saline) as described previously (23, 31). HC-030031 (100 mg/kg i.g.) or its vehicle (0.5% CMC i.g.) and the tachykinin NK_1 receptor antagonist, L-733,060 (2 μmol/kg i.v.; Tocris, Bristol, UK) or its vehicle (isotonic saline) were administered 60 or 15 min before the stimulus, respectively. In a further study, anesthetized (sodium pentobarbital, 50 mg/kg i.p.) *Trpa1*$^{+/+}$ or *Trpa1*$^{-/-}$ mice received Evans blue dye (30 mg/kg i.v.), 1 min before intratracheal instillation (30 μl) of NAPQI (1 mM) or its vehicle (2% DMSO in isotonic saline). NAPQI or vehicle was given in rats and mice through the intratracheal route after exposing the trachea and by inserting a 30-gauge needle just below the inferior laryngeal rim. Animals were euthanized 15 min after NAPQI administration and transcardially perfused with 0.9% isotonic saline solution. The extravasated dye was extracted from rat or mouse trachea and rat conjunctiva by overnight incubation in formamide and assayed by spectrophotometry at 620 nm, as reported previously (23).

Ear edema

Both ear surfaces of anesthetized (5 mg/kg xylazine i.m. and 100 mg/kg ketamine i.p.) C57BL/6, *Trpa1*$^{+/+}$, or *Trpa1*$^{-/-}$ mice were smeared with 1% allyl isothiocyanate or 5 mM NAPQI (20 μl, each side) or their vehicles (paraffin oil and 10% DMSO plus 20% Solutol in isotonic saline, respectively). One ear, chosen at random, was treated with the stimulus or the vehicle in each animal. HC-030031 (300 mg/kg i.g.) or a combination of L-733,060 and the selective CGRP receptor antagonist, $CGRP_{8-37}$ (both 2 μmol/kg i.v.) or their vehicles (0.5% CMC and isotonic saline, respectively) were administered 60 and 15 min before the stimulus, respectively. Ear thickness was measured with an engineer's micrometer (Harvard Apparatus, Edenbridge, Kent, UK) with 0.01-mm accuracy, before and after (15, 30, 45, and 60 min) the challenge with the test agent by an investigator masked to treatment. Data are expressed as percentage increase in baseline value.

Immunohistochemistry

NAPQI (30 μl; 1 mM) or its vehicle (30 μl; 10% DMSO in isotonic saline) was intratracheally instilled in anesthetized

(sodium pentobarbital, 50 mg/kg i.p.) C57BL/6, *Trpa1*$^{+/+}$, or *Trpa1*$^{-/-}$ mice. After 60 min, mice were euthanized, and tracheas were collected. Tracheas and livers were collected from euthanized mice 90 min after administration of APAP (15, 60, 100, or 300 mg/kg i.p. or 300 mg/kg i.g.) or its vehicle (5% DMSO in warmed isotonic saline or 20% Solutol in distilled water). Some C57BL/6 mice were pretreated with HC-030031 (300 mg/kg i.g.) or a combination of L-733,060 and $CGRP_{8-37}$ (both 2 μmol/kg i.v.) or their vehicles (0.5% CMC and isotonic saline, respectively) that were administered 60 and 15 min before the stimulus, respectively. In another set of experiments C57BL/6 mice were pretreated with BSO (800 mg/kg i.p.) or its vehicle (isotonic saline) 1 h before administration of APAP (15 mg/kg i.p.) or its vehicle (5% DMSO in warmed isotonic saline) or the pretreatment with HC-030031 (300 mg/kg i.g.) or its vehicle (0.5% CMC). After the various treatments, mice were transcardially perfused, and tracheas and livers were removed en bloc and fixed in 10% formalin, then paraffin-embedded for immunohistochemical analysis following standard procedures. Endogenous peroxidase activity was blocked by treating the sections with 3% hydrogen peroxide for 10 min. After blocking with normal horse serum (UltraVision; LabVision, Fremont, CA, USA), sections were incubated with an anti-mouse monoclonal neutrophil elastase antibody (dilution 1:200; Santa Cruz Biotechnology, Santa Cruz, CA, USA) for 30 min at room temperature. Staining was performed using avidin-biotin-peroxidase (ABC) (LabVision). Signal was detected using 3.3′-diaminobenzidine (LabVision) as chromogen. Nuclei were counterstained with Mayer's hematoxylin. Negative controls were obtained by substituting the primary antibody with a nonimmune serum. After selection at low-power magnification of more densely immunopositive areas, quantification of neutrophil elastase-positive cells was done in 6 to 8 random high-power fields (HPFs; ×400). An expert pathologist, masked to the experimental group, counted positively stained neutrophils emigrated into the extravascular space (in tracheal tissues both in the epithelium and subepithelial chorion) (32). The results are expressed as mean number/HPF.

Myeloperoxidase (MPO) activity assay

Tracheas and bronchi were collected from euthanized C57BL/6, *Trpa1*$^{+/+}$, or *Trpa1*$^{-/-}$ mice 90 min or 24 h after administration of APAP (15, 60, 100, or 300 mg/kg i.p. or i.g.) or its vehicle (5% DMSO in warmed isotonic saline or 20% Solutol in distilled water, respectively). Some C57BL/6 mice were pretreated with HC-030031 (300 mg/kg i.p.) or a combination of L-733,060 and $CGRP_{8-37}$ (both 2 μmol/kg i.v.) or their vehicles (0.5% CMC and isotonic saline, respectively) 60 and 15 min before the stimulus, respectively. In another set of experiments C57BL/6 mice were pretreated with BSO (800 mg/kg i.p.) or its vehicle (isotonic saline) 60 min before administration of APAP (15 mg/kg i.p.) or its vehicle (5% DMSO in warmed isotonic saline). Livers were also collected from C57BL/6 mice 90 min after administration of APAP (300 mg/kg i.p.) or its vehicle. Ears were also collected from *Trpa1*$^{+/+}$ or *Trpa1*$^{-/-}$ mice 90 min after systemic administration of APAP (60 or 300 mg/kg i.p.) or its vehicle. The MPO activity was assayed as described previously (33). The enzyme activity was evaluated as absorbance at 630 nm. Values are expressed as OD, corrected by g of tissue.

Inflammatory mediator determination

Tracheas and bronchi were collected from euthanized C57BL/6, *Trpa1*$^{+/+}$, or *Trpa1*$^{-/-}$ mice 360 min and 24 h after administration of APAP (60 mg/kg i.p. or i.g.) or its vehicle (5% DMSO in warmed isotonic saline or 20% Solutol in distilled water, respectively). Samples were homogenized in ice-cold lysis buffer (PBS plus Complete Mini Protease Inhibitor Cocktail; Roche, Milan, Italy), and lysates were assessed for total protein content using a Bradford assay (Pierce, Rockford, IL, USA). Levels of monocyte chemotactic protein-1 (MCP-1), IL-1β, keratinocyte chemoattractant (KC), and TNF-α in the lysates were determined by ELISAs using commercial kits (Arcus Biologicals, Modena, Italy) according to the manufacturer's instructions. Data are expressed as pg of cytokine/mg of protein.

Bronchoalveolar lavage

The bronchoalveolar lavage fluid (BALF) was collected from anesthetized (sodium pentobarbital, 50 mg/kg i.p.) C57BL/6 mice 90 min or 6 h after APAP (300 mg/kg i.p.) administration or its vehicle (5% DMSO in warmed isotonic saline). Lungs were lavaged by instilling 0.6 ml of Hanks' buffer plus 10 mM HEPES and 10 mM EDTA 3 times. Routine BALF recovery averaged ~80% of instilled volume. Total cells and neutrophil count were obtained by using an automatic cell analyzing system (Sysmex; Dasit, Cornaredo, Italy). Differential cell counts were obtained using standard morphological criteria on Diff-Quick-stained cytospins. Data are expressed as percentage of number of neutrophils.

3′-GS-APAP adduct analysis by liquid chromatography–electrospray ionization–tandem mass spectrometry (LC-ESI-MS/MS)

Lung and liver tissues, obtained from C57BL/6 mice euthanized from 5 to 90 min after APAP administration (15–300 mg/kg i.p.), were processed for analysis of the 3′-GS-APAP adduct. Lung and liver tissues were homogenized in cold PBS (1:4, w/v) and then centrifuged at 9000 *g* for 20 min at 4°C. Aliquots of S9000 fractions (500 μl) were spiked with the internal standard (IS; 20 μM final concentration), deproteinized by addition of 500 μl of 700 mM perchloric acid solution, and vortex-mixed for 1 min. After 15 min at 4°C, the samples were centrifuged at 21,000 *g* for 10 min. The supernatants were diluted (1:1, v/v) with the mobile phase and filtered through 0.2-μm nylon filters, and the filtrates were transferred to the autosampler vial insert (10-μl samples injected). For *in vitro* experiments, S9000 liver and lung fractions from control animals were incubated with APAP (10 μM final concentration) at 37°C for different time periods (0, 5, 15, 30, 60, and 90 min) and then were processed as reported above. Stability of 3′-GS-APAP in the biological matrices was checked by incubating the compound up to 90 min in the lung and liver S9000 fractions (recovery was more than 98%). Analyses were performed using a Surveyor LC system equipped with a quaternary pump, a Surveyor autosampler, and a vacuum degasser and connected to a TSQ quantum triple quadrupole mass spectrometer (Thermo Finnigan, Milan, Italy). Chromatographic separations were done by reverse-phase elution with a Synergi Polar-RP column (150×2 mm i.d.; particle size 4 μm; Chemtek Analytica, Bologna, Italy) protected by a Polar-RP guard column (4 mm×2 mm i.d.; 4 μm) kept at 30°C. The mass spectrometer was equipped with an ESI interface, which was operated in the positive-ion mode and controlled by Xcalibur 1.4 software (Thermo Finnigan). Separations were done by gradient elution from 100% phase A (90% H_2O/10% CH_3CN/0.1% heptafluorobutyric acid) to 60% phase B (CH_3CN) in 20 min at a flow

rate of 0.2 ml/min (injection volume 10 μl); the composition of the eluent was then restored to 100% A within 2 min, and the system was reequilibrated for 6 min. The samples rack was maintained at 4°C. ESI interface parameters (positive-ion mode) were set as follows: middle position; capillary temperature 270°C; and spray voltage 4.5 kV. Nitrogen was used as the nebulizing gas at the following pressure: sheath gas 30 psi; auxiliary gas 5 arbitrary units. Mass spectrometry tuning was performed by mixing the water-diluted stock solutions of analytes through a T connection (flow rate 10 μl/min), with the mobile phase maintained at a flow rate of 0.2 ml/min; the intensity of the $[M+H]^+$ ions was monitored and adjusted to the maximum by using Quantum Tune Master software (Thermo Finnigan). Quantization was performed in multiple reaction monitoring (MRM) mode at 2.00-kV multiplier voltage; the following MRM transitions of $[M+H]^+$ precursor ion → product ions were selected for each analyte, and the relative collision energies were optimized by the Quantum Tune Master software: H-Tyr-His-OH (IS) m/z 319.2 → 156.5 + 301.6 (collision energy 25 eV).

Statistical analysis

Data are presented as means ± SE or confidence interval (CI). Agonist potency was expressed as EC_{50}, that is, the molar concentration of agonist producing 50% of the measured effect. ANOVA followed by the *post hoc* Bonferroni's test was used for comparisons of multiple groups and the unpaired 2-tailed Student's t test was used for comparisons between 2 groups. Values of $P < 0.05$ were considered significant.

RESULTS

NAPQI selectively activates the recombinant and the native TRPA1 channel

In rTRPA1-HEK293, but not in the vector-HEK293, the TRPA1 agonist cinnamaldehyde and the reactive compound NAPQI (22) (**Fig. 1*A***), caused a concentration-

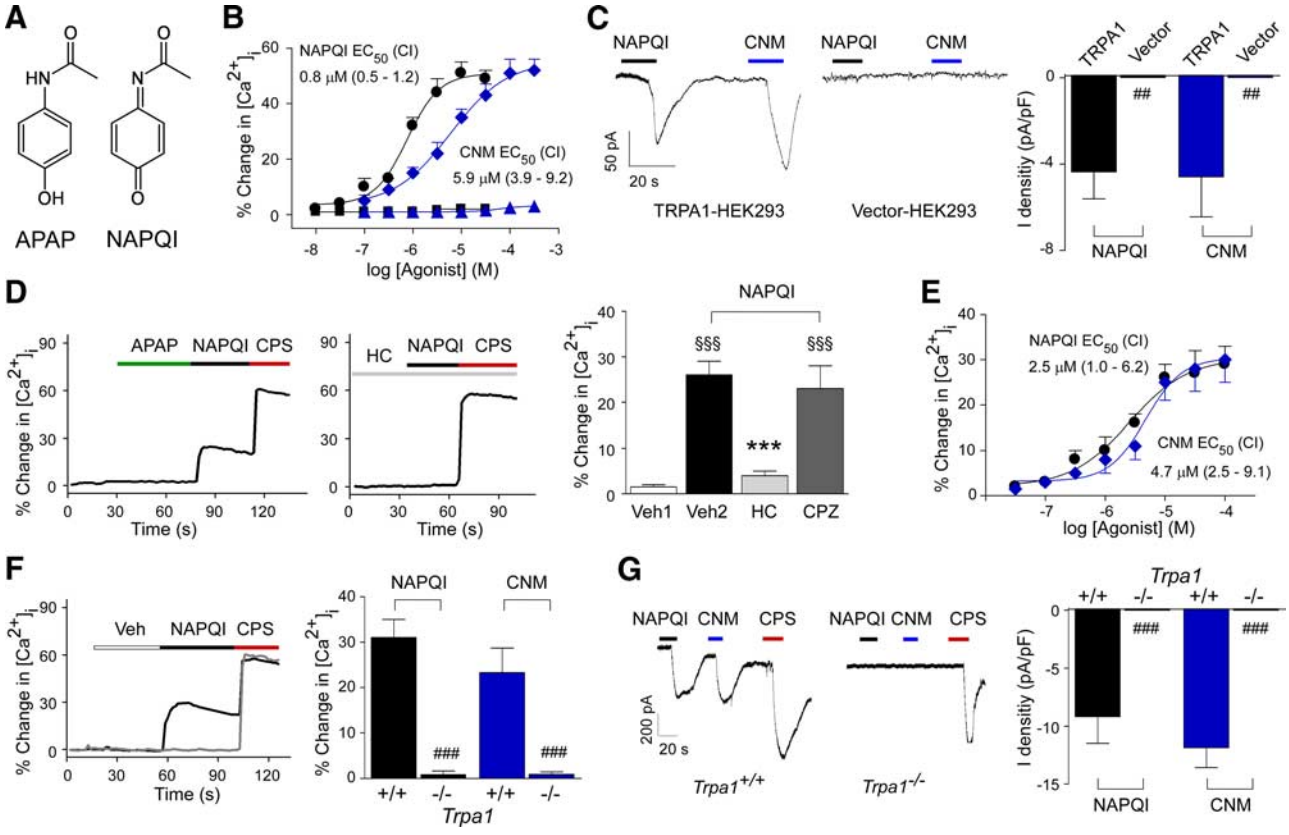

Figure 1. NAPQI selectively signals the recombinant and the native rodent TRPA1 channel. *A*) Chemical structures of APAP and NAPQI. *B*) Concentration-response curves and EC_{50} (CI) values of NAPQI (black circles) and of the selective TRPA1 agonist cinnamaldehyde (CNM; blue diamonds) in rTRPA1-HEK293 cells. NAPQI (black squares) and CNM (blue triangles) did not induce any response in vector-HEK293 cells; $n > 25$ cells. *C*) Representative traces and pooled data of current densities evoked by NAPQI (10 μM) or CNM (10 μM) in patch-clamped rTRPA1-HEK293 cells (TRPA1); $n = 6–7$ cells. No response is observed in vector-HEK293 cells (vector). $^{\#\#}P < 0.01$ *vs.* rTRPA1-HEK293. *D*) NAPQI (10 μM), but not APAP (100 μM), evokes a calcium response in cultured rat JG neurons, sensitive to capsaicin (CPS; 1 μM); $n > 24$ neurons. The response is abolished by HC-030031 (HC; 30 μM), but not by the selective TRPV1 antagonist, capsazepine (CPZ; 10 μM). Veh1, vehicle of NAPQI; Veh2, combination of vehicles of HC-030031 and capsazepine. $^{\S\S\S}P < 0.001$ *vs.* Veh1; $^{***}P < 0.001$ *vs.* Veh2. *E*) Concentration-response curves and EC_{50} (CI) values of NAPQI and CNM (black circles and blue diamonds, respectively) in rat JG neurons; $n > 24$ neurons. *F*) Calcium mobilization induced by NAPQI (10 μM) and CNM (30 μM) in CPS-sensitive DRG neurons isolated from wild-type (*Trpa1*$^{+/+}$, black line) or TRPA1-deficient (*Trpa1*$^{-/-}$, gray line) mice; $n > 24$ neurons. *G*) Current densities evoked by NAPQI (10 μM), CNM (10 μM), and CPS (0.1 μM) in patch-clamped DRG neurons isolated from *Trpa1*$^{+/+}$ or *Trpa1*$^{-/-}$ mice; $n = 10–13$ neurons. Veh, vehicle of NAPQI. $^{\#\#\#}P < 0.001$ *vs.* *Trpa1*$^{+/+}$. Values are means ± SE.

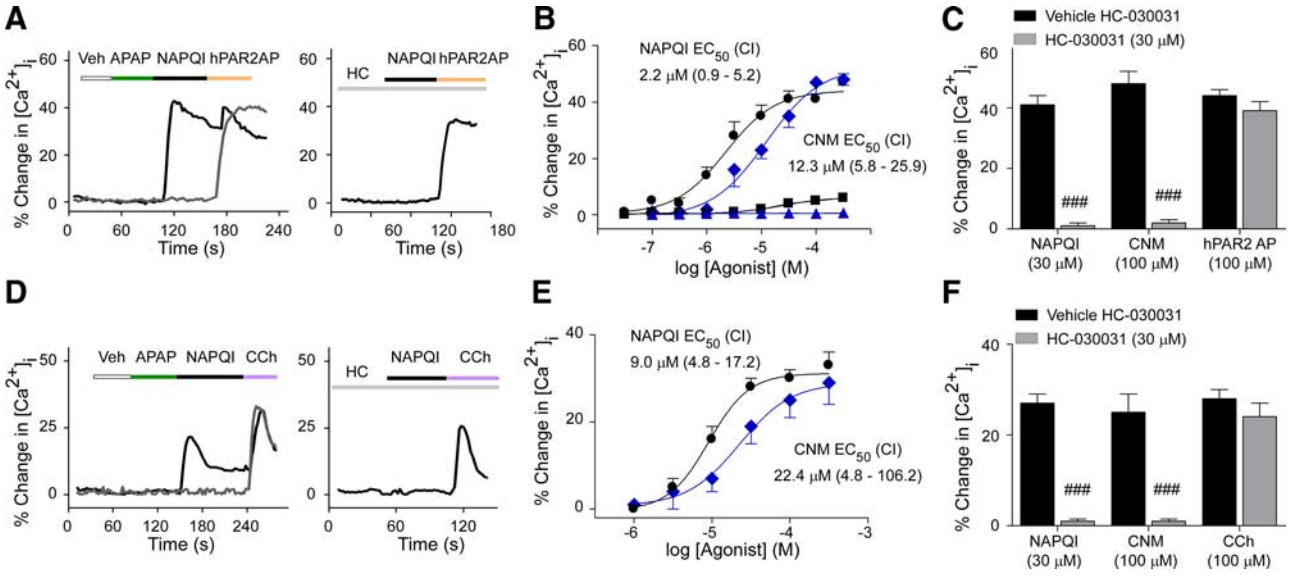

Figure 2. NAPQI, but not APAP, selectively signals the recombinant and the native human TRPA1 channel. Representative traces (*A*) and concentration-response curves (*B*) with EC_{50} (CI) values evoked by NAPQI (black circles) and the selective TRPA1 agonist cinnamaldehyde (CNM; blue diamonds) in hTRPA1-HEK293 cells. *A, C*) Selective TRPA1 antagonist HC-030031 abolishes responses induced by NAPQI or CNM, but not the effect induced by the activating peptide of hPAR-2 AP. *A, B*) In untransfected HEK293 cells (gray line), NAPQI (black squares) and CNM (blue triangles) do not induce any response. *D, E*) In differentiated human neuroblastoma (IMR-32) cells, which express TRPA1, NAPQI and CNM increase intracellular calcium in a concentration-related manner. *D*) In nondifferentiated IMR-32 cells, NAPQI does not induce any effect (gray line). *D, F*) Calcium responses evoked by NAPQI or CNM, but not that induced by carbachol (CCh), are abolished by HC-030031. *A, D*) In both cell types expressing the TRPA1 channel, APAP (100 μM) does not evoke any calcium response. Values are means ± SE; $n > 30$ cells. Veh, vehicle of NAPQI. $^{###}P < 0.001$ *vs.* vehicle HC-030031.

dependent elevation of intracellular calcium (Fig. 1*B*). NAPQI and cinnamaldehyde also activated both hTRPA1-KEK293 cells (**Fig. 2*A, B***) and differentiated IMR-32 human neuroblastoma cells (Fig. 2*D, E*), which have been previously reported to express the TRPA1 channel (27). Calcium responses to NAPQI and cinnamaldehyde in human TRPA1 were abated by HC-030031 (Fig. 2*A, C, D, F*). In hTRPV1-HEK293 cells, which responded to capsaicin, NAPQI was ineffective (data not shown). NAPQI and cinnamaldehyde evoked a large fast inactivating inward membrane current in rTRPA1-HEK293 but not in Vector-HEK293 cells (Fig. 1*C*). APAP did not evoke any calcium response in either hTRPA1-HEK293 and rTRPA1-HEK293 cells (Fig. 2*A* and data not shown, respectively) or neuroblastoma cells (Fig. 2*D*). Thus, NAPQI, but not its precursor, APAP, selectively and potently activates the recombinant TRPA1 channel.

NAPQI, but not APAP, evoked a calcium response in cultured rat JG sensory neurons, which constitutively express TRPA1 (23) with a potency similar to that of cinnamaldehyde (Fig. 1*E*). The response to NAPQI was inhibited by HC-030031 but was unaffected by the TRPV1 antagonist, capsazepine (Fig. 1*D*). Both NAPQI and cinnamaldehyde caused a calcium response in cultured DRG neurons isolated from wild-type mice, which also responded to capsaicin (Fig. 1*F*), indicating coexpression of TRPA1 with TRPV1. In contrast, DRG neurons taken from TRPA1-deficient mice, which responded to capsaicin normally, completely failed to respond to both NAPQI and cinnamaldehyde (Fig. 1*F*). In neurons from wild-type mice, NAPQI or cinnamaldehyde evoked large, fast inactivating inward membrane currents, whereas in neurons taken from TRPA1-deficient mice the currents were completely absent (Fig. 1*G*). Thus, pharmacologic and genetic findings demonstrate that NAPQI, but not APAP, selectively excites native TRPA1 expressed by JG and DRG primary sensory neurons, thus promoting a marked increase in intracellular calcium.

NAPQI evokes the release of sensory neuropeptides that mediate neurogenic inflammatory responses in the airways

Because the TRPA1 agonists 4-hydroxy-2-nonenal and acrolein elicit a calcium-dependent release of CGRP and SP from peripheral tissues (19, 23), we reasoned that NAPQI should release neuropeptides from airway sensory nerves. Indeed, NAPQI increased baseline outflow of both SP and CGRP from slices of rat trachea and bronchi in a concentration-related manner. The response evoked by the highest NAPQI concentration was markedly (>80%) inhibited by *in vitro* capsaicin desensitization or by a calcium-free medium (**Fig. 3*A***). Thus, NAPQI evokes a calcium-dependent neurosecretion process from capsaicin-sensitive airway sensory neurons. CGRP receptor activation promotes arterial vasodilatation (34), whereas tachykinin NK_1 receptor activation increases vascular permeability (35). Both mechanisms contribute to plasma protein extravasation and neutrophil migration into the extravascular space (35, 36). In addition, tachykinin NK_2/

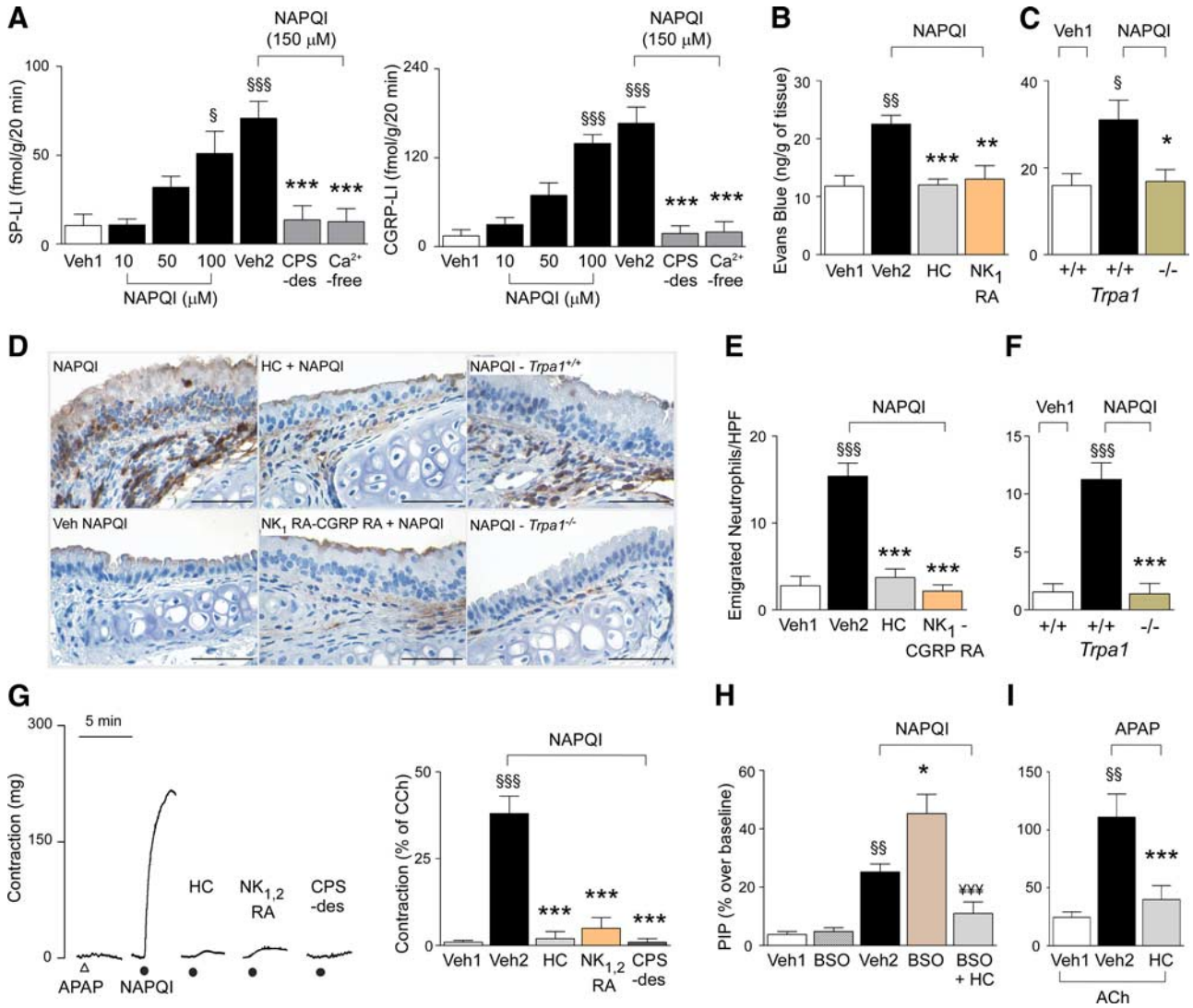

Figure 3. NAPQI releases sensory neuropeptides, thereby inducing neurogenic inflammation *via* TRPA1. *A*) NAPQI increases the release of both SP-like immunoreactivity (SP-LI) and CGRP-like immunoreactivity (CGRP-LI) from rat airway slices in a concentration-dependent manner. Release of both SP-LI and CGRP-LI induced by NAPQI (150 μM) is abolished by capsaicin desensitization (CPS-des) or calcium removal from the medium (Ca^{2+}-free); n = 5–6 experiments. *B*) Plasma protein extravasation evoked by instillation of NAPQI (1 mM, 200 μl) in rat trachea is abolished by HC-030031 (HC; 100 mg/kg i.g.) or by the tachykinin NK_1 receptor antagonist L-733,060 (NK_1-RA; 2 μmol/kg i.v.); n = 5–7 rats. *C*) Plasma protein extravasation induced by instillation of NAPQI (1 mM, 30 μl) in the trachea of *Trpa1*$^{+/+}$ mice is absent in *Trpa1*$^{-/-}$ mice; n = 4–6 mice/group. *D–F*) Immunohistochemical representative images (*D*) and pooled data of the emigrated neutrophil elastase-positive cells in the mouse tracheal epithelial and subepithelial space 60 min after the intratracheal instillation of NAPQI (1 mM, 30 μl; *E, F*). This effect is abolished by pretreatment with HC-030031 (HC; 300 mg/kg, i.g.) or with a combination of L-733,060 and $CGRP_{8-37}$, the CGRP receptor antagonist (NK_1-CGRP RA; both 2 μmol/kg i.v.; *E*) and is absent in *Trpa1*$^{-/-}$ mice (*F*). n = 6–10 mice (*E*); n = 4–6 mice/group (*F*). *G*) Typical tracings and pooled data of the motor effect of NAPQI (3 μM) (●) and APAP (100 μM; △) in guinea pig isolated bronchi; n = 5–6 experiments.. Contraction evoked by NAPQI is abolished by HC (30 μM), a combination of NK_1 and NK_2 receptor antagonists ($NK_{1,2}$ RA; L-733,060 and SR48968, both 1 μM), or CPS-des. *H*) Instillation of NAPQI (1 mM) into the guinea pig trachea *in vivo* causes an increase in PIP, a response that is further increased after pretreatment with BSO (600 mg/kg i.p.), which depletes GSH levels and is abolished by HC (200 mg/kg i.g.). *I*) Moderate increase in PIP evoked by administration of acetylcholine (ACh; 50 nmol/kg i.v.) is potentiated 90 min after APAP administration (300 mg/kg i.p.), and this potentiation is abated by pretreatment with HC (200 mg/kg, i.g.); n = 5–7 guinea pigs. Values are means ± SE. Veh1, vehicle of NAPQI or APAP; Veh2, combined vehicles of the treatments. $^{\S}P < 0.05$, $^{\S\S}P < 0.01$, $^{\S\S\S}P < 0.001$ *vs.* Veh1; $^{*}P < 0.05$, $^{**}P < 0.01$, $^{***}P < 0.001$ *vs.* Veh2 or NAPQI-*Trpa1*$^{+/+}$; $^{¥¥¥}P < 0.001$ *vs.* BSO/NAPQI.

NK_1 receptors mediate nonadrenergic, noncholinergic neurogenic bronchial contraction (37). Therefore, we challenged the hypothesis that NAPQI may induce neurogenic inflammatory responses mediated by sensory neuropeptides *via* TRPA1 activation. Instillation of NAPQI (intratracheal) almost doubled baseline plasma protein extravasation in the rat trachea, an effect abated by HC-0300031 or by the NK_1 receptor antagonist, L-733,060 (Fig. 3*B*). The increase in tracheal plasma extravasation induced by intratracheal instillation of NAPQI in wild-type

mice was completely absent in TRPA1-deficient mice (Fig. 3*C*).

NK_1 receptors mediate (38) and CGRP receptors exaggerate (36) neurogenic neutrophil tissue infiltration. NAPQI instillation (intratracheal) in mice caused a 5-fold increase in the number of infiltrating neutrophils in the tracheal epithelium and subepithelial space (Fig. 3*D, E*). This response was abolished by HC-030031 or by a combination of L-733,060 and $CGRP_{8-37}$ (Fig. 3*D, E*). Similarly, NAPQI instillation (intratracheal) increased neutrophils by ~5-fold in the trachea of wild-type mice, an effect completely absent in TRPA1-deficient animals (Fig. 3*D, F*). NAPQI, but not APAP, contracted guinea pig isolated bronchial rings by a mechanism sensitive to pharmacological blockade of TRPA1 or tachykinin receptors (Fig. 3*G*). Instillation of NAPQI into the guinea pig trachea *in vivo* caused a moderate increase in PIP, a response that was further increased after pretreatment with BSO, a GSH-depleting agent, and was abolished by HC-030031 (Fig. 3*H*). Thus, early inflammatory responses by NAPQI, including bronchoconstriction, plasma protein leakage, and neutrophil infiltration, are caused by a neurogenic mechanism, mediated by TRPA1 stimulation and the release of neuropeptides from sensory nerve endings.

NAPQI evokes conjunctival and skin neurogenic inflammation

APAP consumption has been associated with an increased risk of eczema and rhinoconjunctivitis (10). Because neurogenic inflammation has been documented in the skin and conjunctiva (16), we hypothesized that NAPQI, *via* the release of sensory neuropeptides, elicits inflammation in these tissues. Topical instillation of NAPQI increased plasma extravasation in the rat conjunctiva, an effect abolished by HC-030031 or L-733,060 (**Fig. 4*A***). Ear smearing with the TRPA1 agonist allyl isothiocyanate, which causes ear edema *via* a neurogenic mechanism (39), or NAPQI induced ear swelling, an effect abolished by HC-030031 or by a combination of NK_1 and CGRP receptor antagonists (L-733,060 and $CGRP_{8-37}$, respectively; Fig. 4*B, C*). Conclusive evidence for the unique role of TRPA1 in cutaneous inflammation elicited by allyl isothiocyanate (Fig. 4*D*) and NAPQI (Fig. 4*E*) was obtained in TRPA1-deficient mice, in which no swelling was produced by either agonist. Thus, application of NAPQI to the skin or conjunctiva causes proinflammatory effects that are entirely mediated by TRPA1.

Systemic administration of APAP generates NAPQI in the mouse lung and causes TRPA1-dependent inflammation in the airways and skin

The major GSH adduct of APAP is formed in the liver by thiolate addition of GSH to the electrophilic C′4 of NAPQI, generating a C′4 thiohemiketal *ipso* adduct, followed by a rapid intramolecular rearrangement to give 3′-GS-APAP (22). Here, we provide for the first time direct evidence for NAPQI generation in the lung. In fact, we measured 3′-GS-APAP adduct formation after incubation (from 5 to 90 min) of mouse lung or liver homogenates with APAP (**Fig. 5*A***). More important, measurable amounts of the 3′-GS-APAP adduct were detected not only in the liver but also in the lung from 5 to 90 min after the administration to mice of therapeutic to toxic (15, 60, and 300 mg/kg i.p.) doses of APAP (Fig. 5*B–E*). A dose (15–300 mg/kg)-dependent neutrophil infiltration and increase in MPO activity were observed in the airways 90 min after the administration of APAP (**Fig. 6*A, B, D***). In contrast, toxic (300 mg/kg i.p.) doses of APAP produced neither hepatic neutrophilia nor liver damage at 90 min from APAP administration (data not shown). BSO pretreatment augmented both airway neutrophilia and MPO activity produced by a low (15 mg/kg i.p.) APAP dose (Fig. 6*F, G*), indicating that GSH deficiency may exaggerate the proinflammatory effects of APAP. APAP administration to guinea pigs *in vivo* did not increase PIP (data not shown). However, the increase in PIP evoked by

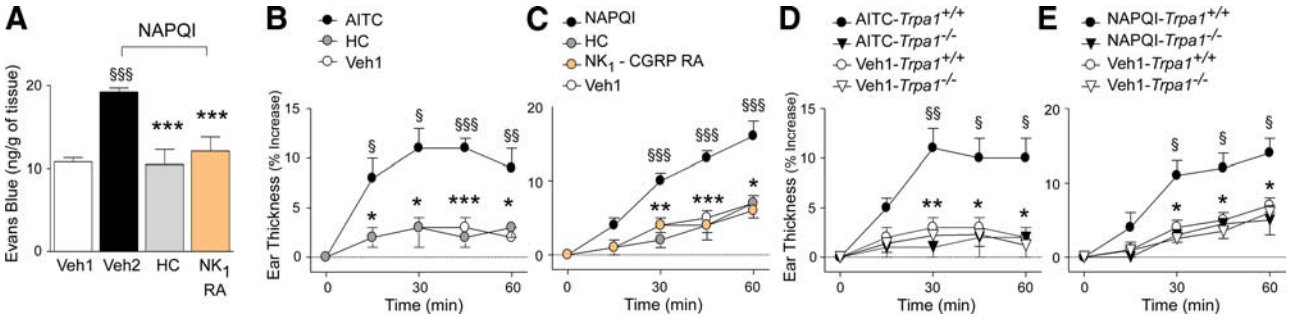

Figure 4. NAPQI evokes skin and conjunctival neurogenic inflammation. *A*) Plasma protein extravasation in rat conjunctiva evoked by topical application of NAPQI (1 mM, 10 μl) is abolished by the pretreatment with HC-030031 (HC; 100 mg/kg i.g.) or the NK_1 receptor antagonist, L-733,060 (NK_1-RA; 2 μmol/kg i.v.); n = 5–7 rats. *B, C*) Ear swelling induced by ear smearing with allyl isothiocyanate (AITC; 1%, 20 μl; *B*) or NAPQI (5 mM, 20 μl; *C*) in C57BL/6 mice is abolished by pretreatment with HC (300 mg/kg i.g.) or by a combination of L-733,060 and $CGRP_{8-37}$ (NK1-CGRP RA; both 2 μmol/kg i.v.); n = 6–10 mice. *D, E*) Ear swelling induced by AITC (1%, 20 μl; *D*) or NAPQI (5 mM, 20 μl; *E*) observed in $Trpa1^{+/+}$ mice is absent in $Trpa1^{-/-}$ mice; n = 4–6 mice/group. Values are means ± SE. Veh1, vehicle of NAPQI or AITC; Veh2, combined vehicles of the treatments. $^{\S}P < 0.05$, $^{\S\S}P < 0.01$, $^{\S\S\S}P < 0.001$ *vs.* Veh1 or Veh1-$Trpa1^{+/+}$; $^{*}P < 0.05$, $^{**}P < 0.01$, $^{***}P < 0.001$ *vs.* Veh2, AITC, in NAPQI, AITC-$Trpa1^{+/+}$, or NAPQI-$Trpa1^{+/+}$.

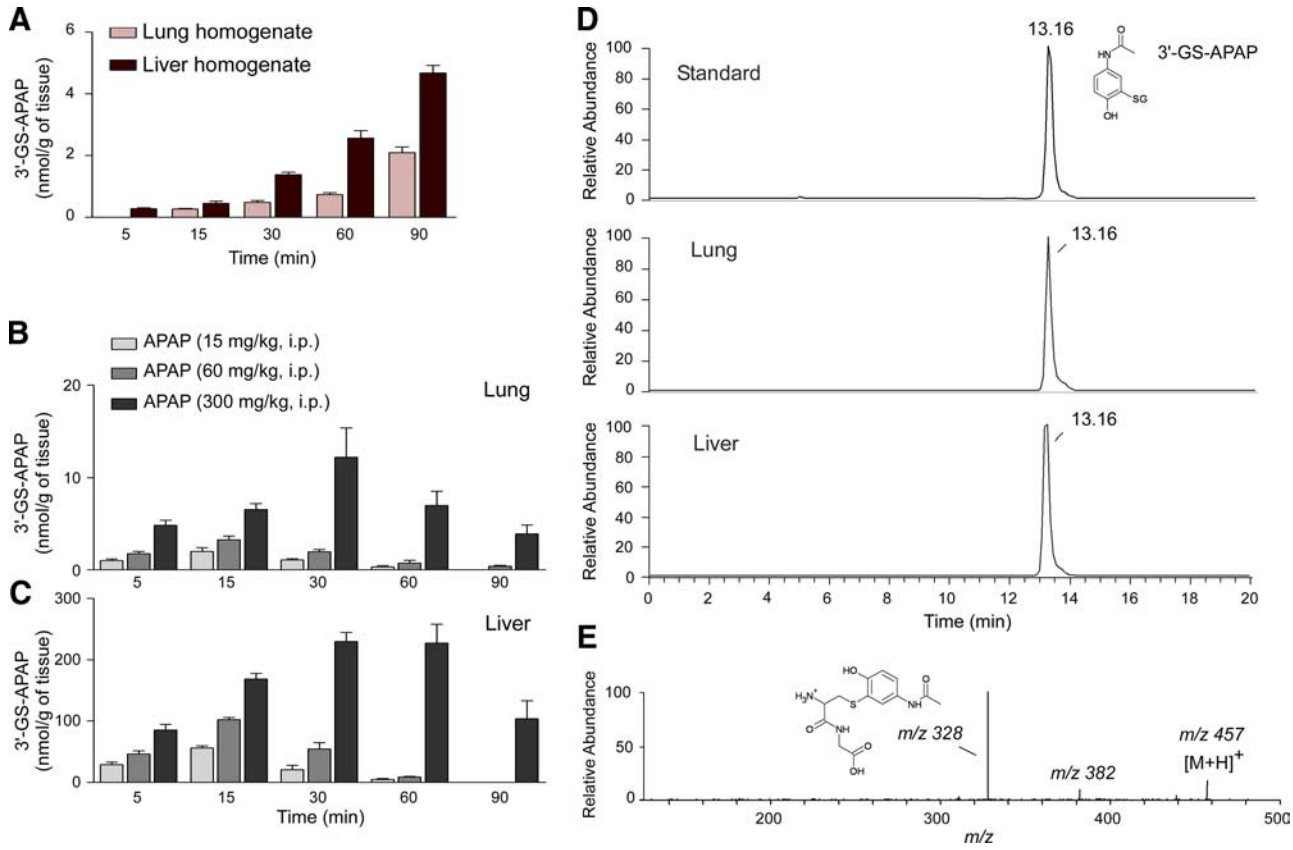

Figure 5. APAP addition to tissue homogenates and systemic APAP administration in mice induces 3′-GS-APAP formation in the lung and liver. *A*) Analysis by LC-ESI-MS/MS of the time course of the formation of the 3′-GS-APAP adduct after *in vitro* addition of APAP (10 μM) to tissue homogenates of mouse lung or liver. Values are means ± SE; $n = 4–5$ experiments. *B*, *C*) Time course of the *in vivo* formation of the 3′-GS-APAP adduct in lung (*B*) and liver (*C*) after systemic administration to mice of 3 different doses of APAP. Values are means ± SE; n = 4–6 mice. *D*) LC-ESI-MS/MS representative traces recorded in MRM mode (parent ion at *m/z* 457.0; product ions at *m/z* 181.9, 328.0, and 382.0) of a standard of 3′-GS-APAP and 3′-GS-APAP generated in lung and liver obtained from mice sacrificed 30 min after *in vivo* APAP (60 mg/kg i.p.) administration. *E*) Product ion spectrum of the precursor ion at *m/z* 457, identified at retention time 13.16 min in the LC-ESI-MS/MS chromatogram carried out in total reaction monitoring mode (parent ion at *m/z* 457.0; *m/z* 50–800 scan range) from lung taken 30 min after APAP (60 mg/kg i.p.) administration.

acetylcholine 90 min after APAP administration was 4-fold higher than the response observed 90 min after the administration of APAP vehicle (Fig. 3*I*). Systemic administration of APAP (60–300 mg/kg i.p.) increased MPO activity in tissue homogenates of the ear of wild-type mice but not of TRPA1-deficient mice (Fig. 6*H*).

APAP (60 mg/kg i.p.) did not affect MCP-1 and IL-1β levels (data not shown), whereas it increased KC (the mouse ortholog of human interleukin-8) and TNF-α levels (Fig. 6*I*, *L*) in airway tissue homogenates of mice, 360 min after drug administration. All the previous APAP-evoked, proinflammatory effects were abolished by HC-030031 or by a combination of NK_1 and CGRP receptor antagonists (Fig. 6*A*, *B*, *D*, *F*, *G*) and were absent in TRPA1-deficient mice (Fig. 6*A*, *C*, *E*). No increase in neutrophils was detected 90–360 min after APAP (60 mg/kg i.p.) in BALF (data not shown). No increase in MPO activity or TNF-α levels in airway tissue homogenates was found 24 h after APAP (60 mg/kg i.p.) administration (data not shown). Thus, airway inflammation induced by administration of low to moderate doses of APAP is mediated by a neurogenic and TRPA1-dependent pathway, most likely caused by NAPQI, and is an early and transient phenomenon, apparently confined to the airway tissue.

APAP proinflammatory activity is maintained after oral administration and does not undergo tachyphylaxis

Because the most common route of APAP administration in humans is oral, we addressed the question whether APAP maintains its proinflammatory effect in the airways after intragastric administration. TRPA1-dependent increases in airway MPO activity, similar to those obtained after intraperitoneal administration of APAP, were observed after intragastric APAP administration (15–300 mg/kg) in mice (**Fig. 7*A*, *B***). APAP (60 mg/kg i.g.) also increased airway TNF-α levels (Fig. 7*D*). To test whether APAP-evoked inflammation is reproducible or undergoes desensitization, we measured two proinflammatory parameters, MPO activity and TNF-α levels, in airway tissue homogenates of mice

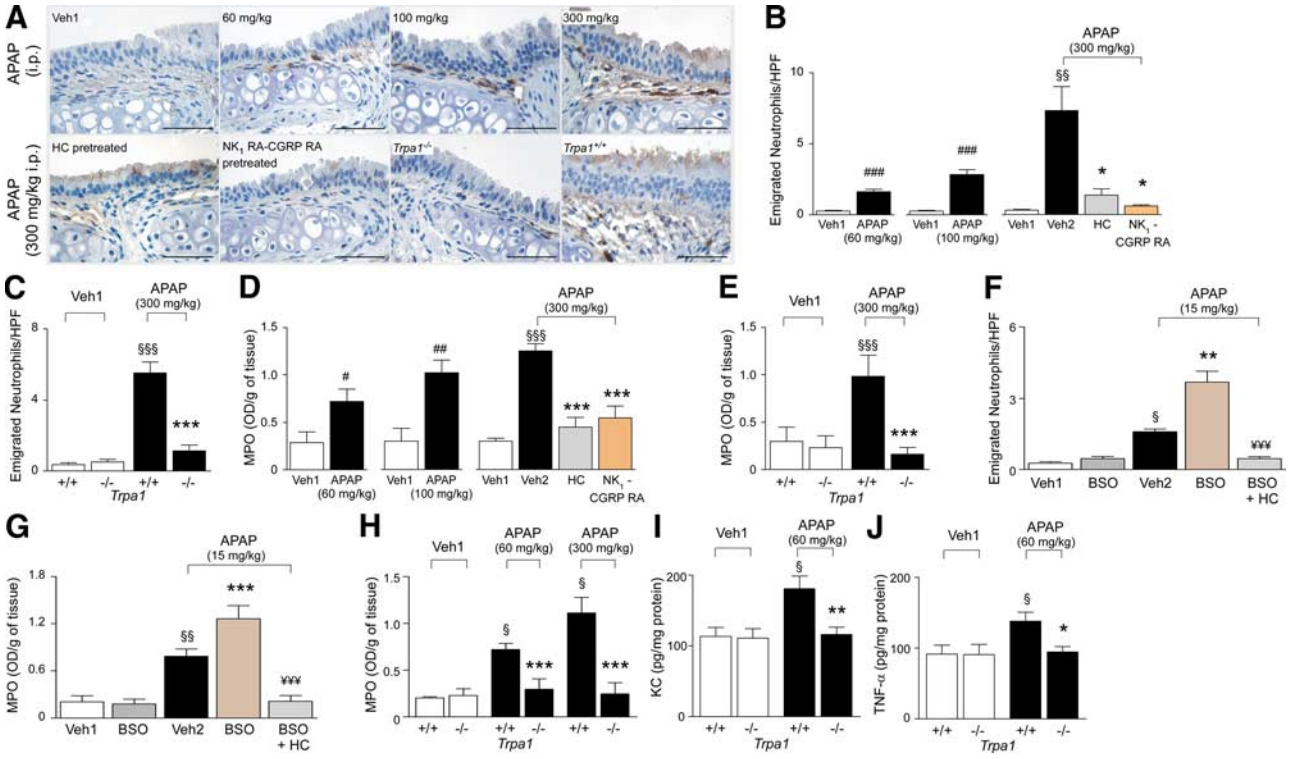

Figure 6. APAP induces airway inflammation by a TRPA1-dependent mechanism in mice. *A–G*) APAP administration to mice increases (90 min after i.p. injection) the number of emigrated neutrophil elastase-positive cells in the tracheal epithelial and subepithelial space (*A*, *B*) and MPO activity in tracheal and bronchial homogenates in a dose-dependent manner (*D*). Both effects are abolished by HC-030031 (HC; 300 mg/kg i.g.) or by a combination of L-733,060 and $CGRP_{8-37}$, NK_1, and CGRP receptor antagonists, respectively (NK_1-CGRP RA; both 2 μmol/kg i.v.) (*A*, *B*, *D*), and absent in *Trpa1*$^{-/-}$ mice (*A*, *C*, *E*). Pretreatment with BSO (800 mg/kg i.p.) increases neutrophil number (*F*) and MPO activity (*G*) evoked by a low dose of APAP (15 mg/kg i.p.), an effect abolished by HC (300 mg/kg i.g.). Values are means ± SE; $n = 6–8$ mice (*B*, *D*, *F*, *G*); $n = 4–10$ mice/group (*C*, *E*). *H*) Systemic APAP administration (i.p.) increases MPO activity in ear tissue homogenates of *Trpa1*$^{+/+}$, an effect completely absent in *Trpa1*$^{-/-}$ mice. Values are means ± SE; $n = 4–10$ mice/group. *I*, *J*) Systemic APAP administration (intraperitoneal) increases tissue levels of KC (*I*) and TNF-α (*J*) (360 min after APAP injection) in tracheal and bronchial homogenates of *Trpa1*$^{+/+}$ mice, an effect completely absent in *Trpa1*$^{-/-}$ mice. Values are means ± SE; $n = 4–10$ mice/group. Veh1, vehicle of APAP; Veh2, combined vehicles of the treatments. $^{\S}P < 0.05$, $^{\S\S}P < 0.01$, $^{\S\S\S}P < 0.001$ *vs.* Veh1 or Veh1-*Trpa1*$^{+/+}$; $^{*}P < 0.05$, $^{**}P < 0.01$, $^{***}P < 0.001$ *vs.* Veh2 or APAP-*Trpa1*$^{+/+}$; $^{¥¥¥}P < 0.001$ *vs.* APAP/BSO; $^{\#}P < 0.05$, $^{\#\#}P < 0.01$, $^{\#\#\#}P < 0.001$ *vs.* Veh1.

treated with APAP (60 mg/kg i.g.) or vehicle after a single treatment (d 1), following two treatments 1 wk apart (*i.e.*, d 1 and 8) or after 3 treatments, each one a week apart (*i.e.*, d 1, 8, and 15). MPO activity was measured in tissues taken from mice sacrificed 90 min after the last intragastric administration of APAP or its vehicle at d 1, 8, or 15. The TNF-α level was measured in tissues taken from mice sacrificed 360 min after the last intragastric administration of APAP or its vehicle at d 1, 8, or 15. Increases in MPO activity or TNF-α level after repeated doses of APAP (2 or 3 times) did not differ significantly from those measured after one dose of the drug, thus indicating absence of desensitization (Fig. 7*C*, *D*).

DISCUSSION

Our data provide strong and unequivocal evidence that the APAP metabolite NAPQI selectively activates the TRPA1 channel expressed in human cells and in rodent sensory neurons. Both pharmacological and genetic findings identify TRPA1 as the target of NAPQI proinflammatory action in the airways and other tissues. We also show that administration of therapeutic doses (including 15 mg/kg, the recommended dose for children) of APAP to mice causes TRPA1-dependent neurogenic inflammatory responses in the airways. In contrast to its metabolite, APAP *per se* does not stimulate TRPA1. The absence in the parent drug of a reactive electrophilic carbon atom, required for TRPA1 activation, and its presence in the oxidized metabolite, NAPQI, is the most plausible reason for the difference. Therefore, APAP must be metabolized to NAPQI to exert the TRPA1-mediated inflammatory effect. Indeed, after systemic administration of therapeutic doses of APAP, we measured detectable levels of NAPQI in the lung. Although the lung has the enzymatic repertoire to generate NAPQI, as demonstrated by the ability of lung tissue homogenates to convert APAP into NAPQI, the present experiments cannot conclusively establish whether NAPQI is entirely produced in the

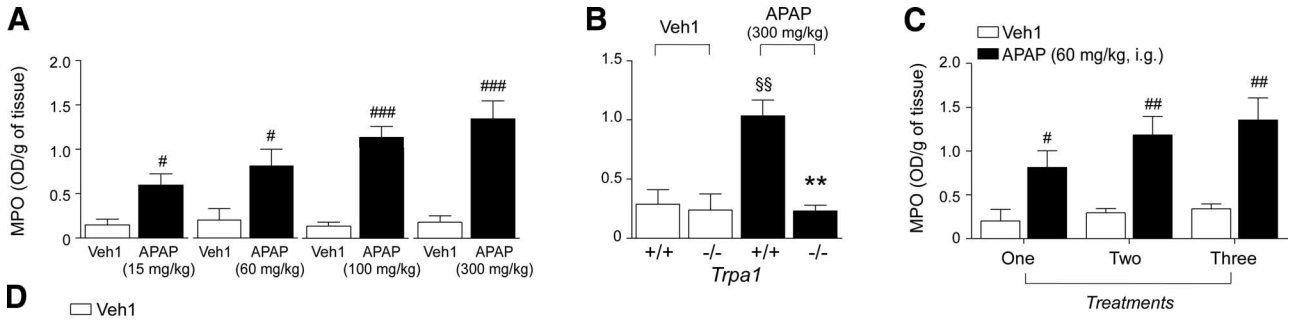

Figure 7. Airway inflammation is induced by oral administration of APAP and does not undergo desensitization. *A*) Dose-dependent increase in MPO activity in mouse tracheal and bronchial homogenates collected 90 min after the i.g. administration of APAP (15–300 mg/kg) or its vehicle; $n = 6–8$ mice. *B*) Increase in MPO activity observed 90 min after the administration of APAP (300 mg/kg i.g.) in *Trpa1*$^{+/+}$ mice is absent in *Trpa1*$^{-/-}$ mice; $n = 4–6$ mice/group. *C*, *D*) MPO activity and TNF-α levels were measured in homogenates of tracheas and bronchi of mice treated with APAP (60 mg/kg i.g.) or vehicle after a single treatment (d 1), following 2 treatments 1 wk apart (*i.e.*, d 1 and 8), or after 3 treatments each 1 wk apart (*i.e.*, d 1, 8, and 15). *C*) MPO activity was measured in tissues taken from mice sacrificed 90 min after the last i.g. administration of APAP or its vehicle at d 1, 8 or 15. *D*) TNF-α level was measured in tissues taken from mice sacrificed 360 min after the last i.g. administration of APAP or its vehicle at d 1, 8, or 15; $n = 6–8$ mice. Increases in MPO activity or TNF-α level after repeated doses of APAP (2 or 3 times) did not differ significantly from those measured after one dose of the drug, thus indicating absence of desensitization. Values are means ± SE. Veh1, vehicle of APAP. $^{§§}P < 0.01$ *vs.* Veh1-*Trpa1*$^{+/+}$; $^{**}P < 0.01$ *vs.* APAP-*Trpa1*$^{+/+}$; $^{\#}P < 0.05$, $^{\#\#}P < 0.01$, $^{\#\#\#}P < 0.001$ *vs.* Veh1.

lung or, at least in part, enters into the lung from the systemic circulation. Irrespective of the origin, we propose that airway inflammation, evoked by APAP, is mediated by its reactive metabolite, NAPQI.

APAP-induced airway inflammation is an early phenomenon, already evident 90 min after APAP administration, at a time when, even after a 300 mg/kg dose, no inflammation or tissue damage is detectable in the liver (40). The transient nature of the response produced by therapeutic doses of APAP is underlined by the observation that increases in MPO activity and TNF-α were no longer seen 24 h after drug administration. The abundant sensory fiber network in the airways, which is absent in the liver, may explain the differential effect. Thus, we hypothesize that the transient response to therapeutic doses of APAP is observed only in highly innervated tissues, whereas noninnervated tissues exhibit solely the delayed, tissue-damaging effect caused by toxic APAP doses. A dense sensory innervation is also present in the skin and conjunctiva, and this may account for the TRPA1-dependent, proinflammatory action produced by NAPQI in both tissues.

The use of APAP has been associated with an increased risk of COPD (7), an inflammatory airway disease characterized by chronic bronchitis and emphysema. The recent observation that α,β-unsaturated aldehydes contained in cigarette smoke (the major causative agent of COPD) produce an inflammatory airway response, which is entirely mediated by neuronal TRPA1 (23), suggests a causal relationship between TRPA1-driven inflammation and COPD. A large series of epidemiological studies has also associated previous use of APAP with the risk of asthma in children and adults (10, 41, 42), although the mechanism by which APAP increases the risk of asthma is unknown. Accidental exposure to a number of environmental irritants has been reported to cause asthma-like symptoms, which have been labeled under various names, including reactive airways dysfunction syndrome (RADS) (43–45), a condition that sometimes outlasts the short-lived exposure to irritants by many years (44). As for NAPQI, many of these substances, including chlorine gas and reactive oxygen species (46), acrolein (18, 23), nitric oxide *via* nitrooleic acid formation (47), isocyanates (48), and toluene diisocyanate (49) are TRPA1 stimulants. In addition, the primary role of TRPA1 in asthma has been strengthened by the recent observation that in mice, pharmacological blockade or genetic deletion of the TRPA1 channel diminishes allergen-induced airway inflammation and hyperreactivity (50). Although several lines of evidence suggest a link between inflammatory chronic airway diseases and TRPA1 activation, it should be underlined that, at present, a satisfactory explanation either for the reason that RADS becomes a chronic condition (44) or for the lengthy delay between APAP exposure and the onset of COPD (7) or asthma (10) is lacking. Nevertheless, our findings provide evidence that APAP *via* NAPQI and TRPA1 activates a specific molecular pathway that may be relevant for human airway inflammatory diseases. In particular, this novel TRPA1-dependent mechanism may provide some explanation for the observed association between the use of APAP and the increased risk of asthma in children (10). The proinflammatory pathway, produced by NAPQI generation and TRPA1 activation, is not limited to the airway tissues, but can also occur at the cutaneous level, as shown by the increase in MPO

activity in the mouse ear after *in vivo* administration of APAP.

Our study reveals a novel, receptor-mediated, neurogenic proinflammatory action of NAPQI, which should be distinguished from the previously known toxic effect of the metabolite. Neurogenic inflammation produced by NAPQI is exquisitely TRPA1-dependent, occurs at therapeutic doses of APAP, and is an early, mild to moderate, and transient phenomenon. In contrast, the toxic effects of NAPQI produced by APAP in overdose involve a number of nonspecific targets, resulting in delayed and serious adverse events (40). Although neurogenic inflammation has long been known as a protective and self-limiting process with no or minimal permanent consequences, in tissues characterized by a dense sensory innervation, repeated exposure to irritant stimuli causes protracted neurogenic inflammatory responses, which may contribute to a chronic disease phenotype (17). Our data show that small quantities of locally generated and nondetoxified NAPQI are sufficient to gate neuronal TRPA1. The resulting mild to moderate inflammatory insult may contribute to the increased risk of asthma and other atopic and inflammatory conditions that are associated with APAP consumption. It may be speculated that individuals, including infants and children, who develop COPD, asthma, eczema, and rhinoconjunctivitis because of APAP consumption (10), are those who, for different reasons, exhibit, persistently or temporarily, an insufficient detoxifying system, mainly represented by GSH (2), which fails to efficiently counteract TRPA1 activation by the APAP metabolite, NAPQI. FJ

The authors are grateful to David Julius (University of California, San Francisco, CA, USA) for TRPA1 heterozygous mice, and to Marco Marchi (University of Florence, Florence, Italy) for advice on statistical analysis. This work was supported by grants from Ministero dell'Istruzione, dell'Università e della Ricerca, Rome (Fondo per gli Investimenti della Ricerca di Base, RBIP06YM29 to P.G. and R.P.), Programmi di Ricerca di Interesse Nazionale (2003054380), Ente Cassa di Risparmio di Firenze (to P.G), and Fondazione Amici Facoltà di Medicina di Firenze (to P.G).

REFERENCES

1. Arrowsmith, J. B., Kennedy, D. L., Kuritsky, J. N., and Faich, G. A. (1987) National patterns of aspirin use and Reye syndrome reporting, United States, 1980 to 1985. *Pediatrics* **79,** 858–863
2. Dahlin, D. C., Miwa, G. T., Lu, A. Y., and Nelson, S. D. (1984) *N*-Acetyl-*p*-benzoquinone imine: a cytochrome P-450-mediated oxidation product of acetaminophen. *Proc. Natl. Acad. Sci. U. S. A.* **81,** 1327–1331
3. Shaheen, S. O., Newson, R. B., Sherriff, A., Henderson, A. J., Heron, J. E., Burney, P. G., and Golding, J. (2002) Paracetamol use in pregnancy and wheezing in early childhood. *Thorax* **57,** 958–963
4. Del-Rio-Navarro, B. E., Luna-Pech, J. A., Berber, A., Zepeda-Ortega, B., Avila-Castanon, L., Del-Rio-Chivardi, J. M., Baeza-Bacab, M., and Sienra-Monge, J. J. (2007) Factors associated with allergic rhinitis in children from northern Mexico City. *J. Investig. Allergol. Clin. Immunol.* **17,** 77–84
5. Shaheen, S. O., Sterne, J. A., Songhurst, C. E., and Burney, P. G. (2000) Frequent paracetamol use and asthma in adults. *Thorax* **55,** 266–270
6. Barr, R. G., Wentowski, C. C., Curhan, G. C., Somers, S. C., Stampfer, M. J., Schwartz, J., Speizer, F. E., and Camargo, C. A., Jr. (2004) Prospective study of acetaminophen use and newly diagnosed asthma among women. *Am. J. Respir. Crit. Care Med.* **169,** 836–841
7. McKeever, T. M., Lewis, S. A., Smit, H. A., Burney, P., Britton, J. R., and Cassano, P. A. (2005) The association of acetaminophen, aspirin, and ibuprofen with respiratory disease and lung function. *Am. J. Respir. Crit. Care Med.* **171,** 966–971
8. Eneli, I., Sadri, K., Camargo, C., Jr., and Barr, R. G. (2005) Acetaminophen and the risk of asthma: the epidemiologic and pathophysiologic evidence. *Chest* **127,** 604–612
9. Allmers, H., Skudlik, C., and John, S. M. (2009) Acetaminophen use: a risk for asthma? *Curr. Allergy Asthma Rep.* **9,** 164–167
10. Beasley, R., Clayton, T., Crane, J., von Mutius, E., Lai, C. K., Montefort, S., and Stewart, A. (2008) Association between paracetamol use in infancy and childhood, and risk of asthma, rhinoconjunctivitis, and eczema in children aged 6–7 years: analysis from phase three of the ISAAC programme. *Lancet* **372,** 1039–1048
11. Mitchell, J. R., Jollow, D. J., Potter, W. Z., Gillette, J. R., and Brodie, B. B. (1973) Acetaminophen-induced hepatic necrosis. IV. Protective role of glutathione. *J. Pharmacol. Exp. Ther.* **187,** 211–217
12. Newson, R. B., Shaheen, S. O., Chinn, S., and Burney, P. G. (2000) Paracetamol sales and atopic disease in children and adults: an ecological analysis. *Eur. Respir. J.* **16,** 817–823
13. Nuttall, S. L., Williams, J., and Kendall, M. J. (2003) Does paracetamol cause asthma? *J. Clin. Pharm. Ther.* **28,** 251–257
14. Story, G. M., Peier, A. M., Reeve, A. J., Eid, S. R., Mosbacher, J., Hricik, T. R., Earley, T. J., Hergarden, A. C., Andersson, D. A., Hwang, S. W., McIntyre, P., Jegla, T., Bevan, S., and Patapoutian, A. (2003) ANKTM1, a TRP-like channel expressed in nociceptive neurons, is activated by cold temperatures. *Cell* **112,** 819–829
15. Nilius, B., Owsianik, G., Voets, T., and Peters, J. A. (2007) Transient receptor potential cation channels in disease. *Physiol. Rev.* **87,** 165–217
16. Geppetti, P., and Holzer, P. (1996) *Neurogenic inflammation*, CRC Press, Boca Raton, FL, USA
17. Geppetti, P., Materazzi, S., and Nicoletti, P. (2006) The transient receptor potential vanilloid 1: role in airway inflammation and disease. *Eur. J. Pharmacol.* **533,** 207–214
18. Bautista, D. M., Jordt, S. E., Nikai, T., Tsuruda, P. R., Read, A. J., Poblete, J., Yamoah, E. N., Basbaum, A. I., and Julius, D. (2006) TRPA1 mediates the inflammatory actions of environmental irritants and proalgesic agents. *Cell* **124,** 1269–1282
19. Trevisani, M., Siemens, J., Materazzi, S., Bautista, D. M., Nassini, R., Campi, B., Imamachi, N., Andre, E., Patacchini, R., Cottrell, G. S., Gatti, R., Basbaum, A. I., Bunnett, N. W., Julius, D., and Geppetti, P. (2007) 4-Hydroxynonenal, an endogenous aldehyde, causes pain and neurogenic inflammation through activation of the irritant receptor TRPA1. *Proc. Natl. Acad. Sci. U. S. A.* **104,** 13519–13524
20. Dalle-Donne, I., Aldini, G., Carini, M., Colombo, R., Rossi, R., and Milzani, A. (2006) Protein carbonylation, cellular dysfunction, and disease progression. *J. Cell. Mol. Med.* **10,** 389–406
21. Hinman, A., Chuang, H. H., Bautista, D. M., and Julius, D. (2006) TRP channel activation by reversible covalent modification. *Proc. Natl. Acad. Sci. U. S. A.* **103,** 19564–19568
22. Chen, W., Shockcor, J. P., Tonge, R., Hunter, A., Gartner, C., and Nelson, S. D. (1999) Protein and nonprotein cysteinyl thiol modification by *N*-acetyl-*p*-benzoquinone imine via a novel ipso adduct. *Biochemistry* **38,** 8159–8166
23. Andre, E., Campi, B., Materazzi, S., Trevisani, M., Amadesi, S., Massi, D., Creminon, C., Vaksman, N., Nassini, R., Civelli, M., Baraldi, P. G., Poole, D. P., Bunnett, N. W., Geppetti, P., and Patacchini, R. (2008) Cigarette smoke-induced neurogenic inflammation is mediated by α,β-unsaturated aldehydes and the TRPA1 receptor in rodents. *J. Clin. Invest.* **118,** 2574–2582
24. Cottrell, G. S., Padilla, B., Pikios, S., Roosterman, D., Steinhoff, M., Grady, E. F., and Bunnett, N. W. (2007) Post-endocytic sorting of calcitonin receptor-like receptor and receptor activity-modifying protein 1. *J. Biol. Chem.* **282,** 12260–12271
25. Sadofsky, L. R., Campi, B., Trevisani, M., Compton, S. J., and Morice, A. H. (2008) Transient receptor potential vanilloid-1-mediated calcium responses are inhibited by the alkylamine

antihistamines dexbrompheniramine and chlorpheniramine. *Exp. Lung. Res.* **34,** 681–693
26. Trevisani, M., Smart, D., Gunthorpe, M. J., Tognetto, M., Barbieri, M., Campi, B., Amadesi, S., Gray, J., Jerman, J. C., Brough, S. J., Owen, D., Smith, G. D., Randall, A. D., Harrison, S., Bianchi, A., Davis, J. B., and Geppetti, P. (2002) Ethanol elicits and potentiates nociceptor responses via the vanilloid receptor-1. *Nat. Neurosci.* **5,** 546–551
27. Louhivuori, L. M., Bart, G., Larsson, K. P., Louhivuori, V., Nasman, J., Nordstrom, T., Koivisto, A. P., and Akerman, K. E. (2009) Differentiation dependent expression of TRPA1 and TRPM8 channels in IMR-32 human neuroblastoma cells. *J. Cell. Physiol.* **221,** 67–74
28. Sartiani, L., Cerbai, E., Lonardo, G., DePaoli, P., Tattoli, M., Cagiano, R., Carratu, M. R., Cuomo, V., and Mugelli, A. (2004) Prenatal exposure to carbon monoxide affects postnatal cellular electrophysiological maturation of the rat heart: a potential substrate for arrhythmogenesis in infancy. *Circulation* **109,** 419–423
29. Vargas, M. H., Romero, L., Sommer, B., Zamudio, P., Gustin, P., and Montano, L. M. (1998) Chronic exposure to ozone causes tolerance to airway hyperresponsiveness in guinea pigs: lack of SOD role. *J. Appl. Physiol.* **84,** 1749–1755
30. Griffith, O. W., and Meister, A. (1979) Potent and specific inhibition of glutathione synthesis by buthionine sulfoximine (*S-n*-butyl homocysteine sulfoximine). *J. Biol. Chem.* **254,** 7558–7560
31. Figini, M., Javdan, P., Cioncolini, F., and Geppetti, P. (1995) Involvement of tachykinins in plasma extravasation induced by bradykinin and low pH medium in the guinea-pig conjunctiva. *Br. J. Pharmacol.* **115,** 128–132
32. Krishna, M. T., Springall, D., Meng, Q. H., Withers, N., Macleod, D., Biscione, G., Frew, A., Polak, J., and Holgate, S. (1997) Effects of ozone on epithelium and sensory nerves in the bronchial mucosa of healthy humans. *Am. J. Respir. Crit. Care Med.* **156,** 943–950
33. Suzuki, K., Ota, H., Sasagawa, S., Sakatani, T., and Fujikura, T. (1983) Assay method for myeloperoxidase in human polymorphonuclear leukocytes. *Anal. Biochem.* **132,** 345–352
34. Brain, S. D., Williams, T. J., Tippins, J. R., Morris, H. R., and MacIntyre, I. (1985) Calcitonin gene-related peptide is a potent vasodilator. *Nature* **313,** 54–56
35. Joos, G. F., Germonpre, P. R., and Pauwels, R. A. (2000) Role of tachykinins in asthma. *Allergy* **55,** 321–337
36. Buckley, T. L., Brain, S. D., Rampart, M., and Williams, T. J. (1991) Time-dependent synergistic interactions between the vasodilator neuropeptide, calcitonin gene-related peptide (CGRP) and mediators of inflammation. *Br. J. Pharmacol.* **103,** 1515–1519
37. Bertrand, C., and Geppetti, P. (1996) Tachykinin and kinin receptor antagonists: therapeutic perspectives in allergic airway disease. *Trends Pharmacol. Sci.* **17,** 255–259
38. Baluk, P., Bertrand, C., Geppetti, P., McDonald, D. M., and Nadel, J. A. (1995) NK1 receptors mediate leukocyte adhesion in neurogenic inflammation in the rat trachea. *Am. J. Physiol.* **268,** L263–L269
39. Banvolgyi, A., Pozsgai, G., Brain, S. D., Helyes, Z. S., Szolcsanyi, J., Ghosh, M., Melegh, B., and Pinter, E. (2004) Mustard oil induces a transient receptor potential vanilloid 1 receptor-independent neurogenic inflammation and a non-neurogenic cellular inflammatory component in mice. *Neuroscience* **125,** 449–459
40. Cover, C., Mansouri, A., Knight, T. R., Bajt, M. L., Lemasters, J. J., Pessayre, D., and Jaeschke, H. (2005) Peroxynitrite-induced mitochondrial and endonuclease-mediated nuclear DNA damage in acetaminophen hepatotoxicity. *J. Pharmacol. Exp. Ther.* **315,** 879–887
41. Shaheen, S., Potts, J., Gnatiuc, L., Makowska, J., Kowalski, M. L., Joos, G., van Zele, T., van Durme, Y., De Rudder, I., Wohrl, S., Godnic-Cvar, J., Skadhauge, L., Thomsen, G., Zuberbier, T., Bergmann, K. C., Heinzerling, L., Gjomarkaj, M., Bruno, A., Pace, E., Bonini, S., Fokkens, W., Weersink, E. J., Loureiro, C., Todo-Bom, A., Villanueva, C. M., Sanjuas, C., Zock, J. P., Janson, C., and Burney, P. (2008) The relation between paracetamol use and asthma: a GA2LEN European case-control study. *Eur. Respir. J.* **32,** 1231–1236
42. Etminan, M., Sadatsafavi, M., Jafari, S., Doyle-Waters, M., Aminzadeh, K., and Fitzgerald, J. M. (2009) Acetaminophen use and the risk of asthma in children and adults: a systematic review and metaanalysis. *Chest* **136,** 1316–1323
43. Brooks, S. M., Weiss, M. A., and Bernstein, I. L. (1985) Reactive airways dysfunction syndrome (RADS). Persistent asthma syndrome after high level irritant exposures. *Chest* **88,** 376–384
44. Malo, J. L., L'Archeveque, J., J., Castellanos, L., Lavoie, K., Ghezzo, H., and Maghni, K. (2009) Long-term outcomes of acute irritant-induced asthma. *Am. J. Respir. Crit. Care Med.* **179,** 923–928
45. Dykewicz, M. S. (2009) Occupational asthma: current concepts in pathogenesis, diagnosis, and management. *J. Allergy Clin. Immunol.* **123,** 519–528
46. Bessac, B. F., Sivula, M., von Hehn, C. A., Escalera, J., Cohn, L., and Jordt, S. E. (2008) TRPA1 is a major oxidant sensor in murine airway sensory neurons. *J. Clin. Invest.* **118,** 1899–1910
47. Taylor-Clark, T. E., Ghatta, S., Bettner, W., and Undem, B. J. (2009) Nitrooleic acid, an endogenous product of nitrative stress, activates nociceptive sensory nerves via the direct activation of TRPA1. *Mol. Pharmacol.* **75,** 820–829
48. Bessac, B. F., Sivula, M., von Hehn, C. A., Caceres, A. I., Escalera, J., and Jordt, S. E. (2009) Transient receptor potential ankyrin 1 antagonists block the noxious effects of toxic industrial isocyanates and tear gases. *FASEB J.* **23,** 1102–1114
49. Taylor-Clark, T. E., Kiros, F., Carr, M. J., and McAlexander, M. A. (2008) Transient receptor potential ankyrin 1 mediates toluene diisocyanate-evoked respiratory irritation. *Am. J. Respir. Cell Mol. Biol.* **40,** 756–762
50. Caceres, A. I., Brackmann, M., Elia, M. D., Bessac, B. F., Del Camino, D., D'Amours, M., Witek, J. S., Fanger, C. M., Chong, J. A., Hayward, N. J., Homer, R. J., Cohn, L., Huang, X., Moran, M. M., and Jordt, S. E. (2009) A sensory neuronal ion channel essential for airway inflammation and hyperreactivity in asthma. *Proc. Natl. Acad. Sci. U. S. A.* **106,** 9099–9104

Received for publication April 26, 2010.
Accepted for publication August 5, 2010.